

Controlling the Oxygen Reduction Selectivity of Asymmetric Cobalt Porphyrins by Using Local Electrostatic Interactions

Rui Zhang and Jeffrey J. Warren*

Cite This: <https://dx.doi.org/10.1021/jacs.0c03861>

Read Online

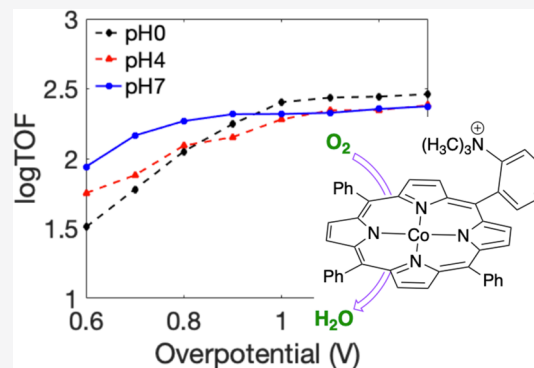
ACCESS |

Metrics & More

Article Recommendations

Supporting Information

ABSTRACT: The development and improvement of electrocatalysts for the $4\text{H}^+/4\text{e}^-$ reduction of O_2 to H_2O is an ongoing challenge. The addition of ancillary groups (e.g., hydrogen bonding, Brønsted acid/base) near the active site of metal-containing catalysts is an effective way to improve selectivity and kinetics of the oxygen reduction reaction (ORR). In this regard, iron porphyrins are among the most researched ORR catalysts. Closely related cobalt porphyrin ORR catalysts can function closer to the $\text{O}_2/\text{H}_2\text{O}$ thermodynamic potential, but they tend to be less selective and follow a different mechanism than for the iron porphyrins. Herein, we explore strategies to extend the ideas about ancillary groups that have been developed for iron porphyrin ORR electrocatalysts to improve the performance of the corresponding cobalt complexes. We describe a series of porphyrin electrocatalysts that are modified versions of Co(5,10,15,20-tetraphenylporphyrin), where the 2-position of one of the phenyl groups contains $-\text{NH}_2$, $-\text{N}(\text{CH}_3)_2$, and $-\text{N}(\text{CH}_3)_3^+$. Investigations using cyclic voltammetry and hydrodynamic electrochemistry show that the presence of a cationic ancillary group gives rise to a catalyst that is selective for the conversion of O_2 to H_2O across a wide pH range. In contrast, the other catalysts are selective for reduction of O_2 to H_2O at pH 0, but produce H_2O_2 at higher pH. The ORR rate ($\sim 10^6 \text{ M}^{-1} \text{ s}^{-1}$) and selectivity of the $-\text{N}(\text{CH}_3)_3^+$ -modified catalyst are invariant between pH 0 and 7. Quantum chemical calculations support the hypothesis that the enhancement of selectivity can be attributed to the distinct mechanism of O_2 reduction by Co-porphyrins. Specifically, the mechanism relies on anionic, peroxide-bound intermediates. While protic ancillary groups are important in the performance of iron porphyrin ORR catalysts, we suggest that electrostatic stabilizers of O_2 -bound intermediates are more crucial for cobalt porphyrin ORR catalysts.



INTRODUCTION

The oxygen reduction reaction (ORR) has been studied for a long time, with emphasis placed on biological reactions^{1–3} and on cathodic reactions in fuel cells.^{4–6} While natural systems use first row metals for ORR chemistry, platinum is primarily used as the catalyst in fuel cells. Improving the adoption of fuel cell technology is closely tied to the identification of an inexpensive and selective catalyst for the ORR. For fuel cell applications, it is particularly important that O_2 reduction involves the 4 electron + 4 proton ($4\text{H}^+/4\text{e}^-$) conversion of O_2 to H_2O . Other pathways, such as those that make superoxide (1e^- reduction) or hydrogen peroxide ($2\text{H}^+/2\text{e}^-$ reduction), are undesirable and can lead to degradation of catalyst systems. With these ideas in mind, the two ongoing challenges for the development of ORR catalysts are (1) to identify nonprecious catalysts and (2) to favor selectivity for O_2 reduction to H_2O .^{4,5} Herein, we describe the systematic investigation of a series of cobalt porphyrin electrocatalysts (Figure 1) that probes how the identity of different ancillary functional groups affect the performance and selectivity for ORR. Of particular interest are differences in the performance of catalysts with

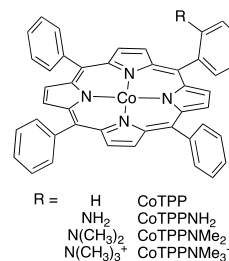


Figure 1. Structures and abbreviations of the cobalt(II) 5-(2-R)-10,15,20-triphenylporphyrins described in this work.

groups that support hydrogen bonding and those that carry a permanent positive charge.

Received: April 8, 2020

To address the two challenges identified above, many different coordination complexes, and especially metalloporphyrin complexes, have been studied.⁷ First row metalloporphyrin ORR catalysts have garnered interest and are a means to satisfy the first of the aforementioned challenges. In particular, many investigations of homogeneous ORR of tetraarylporphyrins have emerged, including work in organic solvents^{8–11} and in aqueous buffers.^{12–14} A unifying theme of many of these reports is that the management of protons and electrons is crucial for selective ORR catalysis, which addresses the second of the above challenges. One important design feature that has received attention is “proton relays.” For ORR catalysis, these are typically Brønsted acids (e.g., carboxylic acids or pyridinium).^{9,13,15,16} Although the explicit roles of these groups during catalysis is debated, and likely depends on reaction conditions,⁷ they appear to play an important role in proton transfer reactions. In addition, there are several examples of catalysts that incorporate multiple metal centers as a means to mediate multiple redox reactions.^{15,17–19} Early multimetallic porphyrin O₂ reduction catalysts were inspired by biological systems, exemplified by cytochrome *c* oxidase active site models.^{20–22} As noted above, a great many other molecular catalyst systems have been developed that have different levels of performance and comprehensive reviews are available.^{7,23}

Iron porphyrin molecular ORR catalysts are among the most widely investigated, in part because they tend to favor reduction of O₂ to H₂O.⁷ The drawback is that they usually function at high overpotentials. We found that, for Fe-porphyrins, graphite adsorption of catalysts, and the incorporation of one proton relay, gave rise robust catalysts for O₂ to H₂O conversion, albeit at overpotentials ≥ 1 V.²⁴ In contrast, Co-porphyrin ORR catalysts can function at lower overpotentials, but favor production of H₂O₂.²⁵ We recently reported that the replacement of one phenyl group of Co(5,10,15,20-tetraphenylporphyrin) (CoTPP) with a 2-pyridyl group dramatically shifted the ORR selectivity from H₂O₂ to O₂ in the case of graphite adsorbed catalysts.²⁶ In related work, Anson and co-workers carried out several investigations of graphite-adsorbed Co-porphyrin ORR catalysts,^{25,27,28} but only some of those molecules or catalyst preparations were selective for reduction of O₂ to H₂O.^{28,29}

Any design of a molecular catalysts must consider the key intermediates in a catalytic cycle.³⁰ The mechanism by which O₂ is reduced by Fe- and Co-porphyrins is likely different at some key reaction steps. In both cases, a reduced metal (M(II)) binds O₂ to give a metal-superoxide complex ([M(III)-O₂^{•-}]ⁿ). For Fe, the pathway likely involves reduction and protonation to yield the corresponding hydroperoxo complex ([M(III)-O₂H]ⁿ). Further reduction and protonation of a ferric-hydroperoxo can yield a formally Fe^{IV}=O complex.³¹ Catalyst-control over proton transfer is especially important for this reaction in iron porphyrin ORR catalysts.³² Co(II) also binds O₂ to form a superoxo complex,^{33–35} but from this point, the mechanisms for Co and Fe diverge. Cobalt porphyrins cannot form stable Co^{IV}-oxo complexes³⁶ and reduction of a Co(III)-O₂^{•-} intermediate has been proposed to give a [Co-OOH⁻] complex during aqueous ORR.³⁷ Protonation of that complex can yield H₂O₂. We note that this reduction sequence is different than has been proposed in homogeneous organic solutions,⁸ but such medium effects can have substantial effects on ORR chemistry.³⁸ The incorporation of proton relays or redox-

active ancillary groups have been investigated in Co-porphyrins, but those designs do not explicitly account for the possibility of an anionic, peroxide-bound intermediates. In this report, we show that a cationic group proximal to the metal in Co-porphyrin ORR catalysts improves selectivity for the 4H⁺/4e⁻ reduction of O₂ across a wide pH range.

Our previous work on Co-porphyrins for ORR²⁶ built upon the idea that proton delivery was crucial for catalyst selectivity, as is the case for Fe-porphyrins.²⁶ However, related work on CO₂ reduction has shown that electrostatic directing groups in iron 5,15,15,20-tetra(trimethylanilinium)porphyrin led to a more dramatic improvement in catalyst activity than did Brønsted acid proton relays.³⁹ That same iron porphyrin also is an O₂ reduction catalyst in MeCN solvent and its unique catalytic properties are tied, in part, to the ability of the cationic porphyrin to bind anions that shift the catalyst reduction potentials.⁴⁰ Given the above examples, the catalytic improvements we observed²⁶ for a Co-porphyrin with a 2-pyridinium group could have been because of proton transfer reactions (i.e., as a proton relay) or due to electrostatic stabilization of anionic intermediates. In the present report, we designed, prepared, and investigated a series of cobalt porphyrins (Figure 1) to systematically probe the relative importance of proton relay activity and electrostatic interactions of pendant groups in ORR catalysis.

EXPERIMENTAL SECTION

Materials and Instrumentation. Reagents were obtained from Sigma-Aldrich unless otherwise noted and used without further purification. Gases were from Praxair Canada. Basal plane and edge plane graphite (BPG and EPG, respectively) electrodes were prepared according to the literature.⁴¹ Mass spectra were collected by using a Bruker microFlex MALDI-TOF mass spectrometer and electrospray ionization mass spectrometry experiments used and Agilent 6210 instrument. UV–visible spectra were recorded using a Cary100Bio spectrophotometer. Elemental analyses (C, H, N) were performed at Simon Fraser University on a Carlo Erba EA 1110 CHN elemental analyzer.

The ligands, 5,10,15,20-tetraphenylporphyrin (H₂TPP) and 5-(2-aminophenyl)-10,15,20-triphenylporphyrin (H₂TPPNH₂), were synthesized using a literature procedure.⁴² Metalation of porphyrins with Co(II)acetate was carried out according to the literature.²⁶ The ligand, 5-(2-N,N-dimethylphenyl)-10,15,20-triphenylporphyrin (H₂TPPNMe₂) was synthesized using modified literature procedures,^{39,42} and its metalation was carried out by refluxing the ligand with excess Co(II)acetate in dimethylformamide (DMF) for 6 h. Finally, CoTPPNMe₂ was reacted with an excess of methyl triflate in DMF in 24 h to yield CoTPPNMe₃⁺. H₂TPPNMe₂, CoTPPNMe₂, and CoTPPNMe₃⁺ were characterized by NMR, mass spectrometry, UV–vis spectroscopy and elemental analysis. Detailed experimental descriptions and characterization data can be found in the Supporting Information (Figures S1–S9).

Electrochemical Methods. A Pine Instruments WaveDriver 20 bipotentiostat was used for electrochemical measurements. Cyclic voltammetry (CV) and controlled potential electrolysis (CPE) measurements used a conventional three-electrode cell, with an edge plane graphite (EPG) working electrode, basal plane graphite (BPG) counter electrode, and a Ag/AgCl (saturated KCl) reference electrode. Rotating disk electrochemistry (RDE) and rotating ring-disk electrochemistry (RRDE) measurements used the Pine Modulated Speed Rotator. Potassium ferricyanide was used as an external standard for heterogeneous experiments and all potentials are reported with respect to the normal hydrogen electrode (NHE). Electrochemical experiments were carried out in solutions with pH values of 0, 4, and 7. Solutions contained 1 M H₂SO₄ and the pH was adjusted using 1 M NaOH.

Computational Methodology. Calculations were performed using the ORCA 4.2.1 *ab initio* quantum chemistry program.^{43,44} Geometry optimizations and single point calculations were carried out using the TPSS functional,⁴⁵ utilizing the RIJCOSX algorithm.⁴⁶ The basis set was def2-TZVP on Co, def2-SVP/def2/J on other atoms^{47,48} and the Becke-Johnson damping scheme was utilized.^{49,50} Metrical parameters calculated for CoTPP are similar to those in experimental X-ray structures.^{51,52} Optimized structures were characterized using vibrational frequency calculations at the same level of theory to confirm that the structures were located at a minimum on the potential energy surface. Single-point energy calculations used the all electron aug-cc-pVTZ basis set^{53,54} in the gas phase and in water solvent using a dielectric continuum model (CPCM).⁵⁵ The total free energy was calculated following Carter et al.⁵⁶ and included thermochemical and entropic contributions. The explicit solvation energy of H⁺ in water ($-270.3 \text{ kcal mol}^{-1}$)⁵⁷⁻⁵⁹ and an empirical value for NHE (4.281 V)⁶⁰ were used in reaction free energy calculations.

RESULTS AND DISCUSSION

The ligand H₂TPPNMe₂ and the complex CoTPPNMe₃⁺ were prepared following literature procedures for closely related complexes.^{39,42} H₂TPP and H₂TPPNH₂ are known ligands. Full characterization data are given in the [Supporting Information](#). The optical spectra of the amine-substituted Co complexes show Soret bands (412 nm) and Q-bands (521 nm) that are similar to those for the parent CoTPP (410 and 527, respectively).⁶¹ We conclude that the inclusion of the amine group does not dramatically affect the electronic structure of the Co-porphyrins with respect to CoTPP. This series of complexes allows for a systematic test of the role of electrostatic interactions versus proton relay effects. At pH 0, CoTPPNH₂ and CoTPPNMe₂ will be protonated (i.e., the conjugate acids, CoTPPNH₃⁺ and CoTPPNMe₂H⁺), but at higher pH they will exist in the neutral form. In contrast, the charge of the trimethylanilinium group in CoTPPNMe₃⁺ is independent of pH.

Homogeneous cyclic voltammetry experiments were first carried out in MeCN solvent (see Supporting Information, [Figure S10](#)). For CoTPP a reversible Co^{III/II} couple was observed at 0.67 V (versus ferrocenium/ferrocene, Cp₂Fe⁺⁰), consistent with the reported value in propionitrile.⁶² The Co^{III/II} potential for CoTPPNH₂ (0.70 V versus Cp₂Fe⁺⁰) is similar to that of CoTPP, but the potentials for CoTPPNMe₂ (0.75 V versus Cp₂Fe⁺⁰) and CoTPPNMe₃⁺ (0.78 V versus Cp₂Fe⁺⁰) are somewhat higher. This is qualitatively consistent with the shift in potential observed for an NMe₃⁺-substituted iron porphyrin.³⁹ The observed values are similar to the reported potentials for a series of Co-tetraarylporphyrin derivatives.⁶³

Next, each of the Co-porphyrins were drop cast on edge plane graphite (EPG) electrodes. CVs were first collected in Ar-sparged electrolyte at pH values of 0, 4, and 7. CVs for all complexes can be found in the [Supporting Information](#). As expected, from studies of other deposited Co-porphyrins the responses are weak.^{25,27,64} The data for CoTPPNMe₃⁺ are shown in [Figure 2](#). CoTPP exhibits a weak, broad wave at 0.55 V versus NHE, consistent with a report for a similar electrode preparation of CoTPP.²⁷ The cathodic peak ($E_{p,c}$) is observed at 0.47 V (pH 0). This wave is pH-dependent, shifting to more negative values as the pH is increased.

A definitive assignment of formal potentials is complicated by the background response from the EPG electrode and poorly defined anodic waves ($E_{p,a}$). Overall, the observed pH

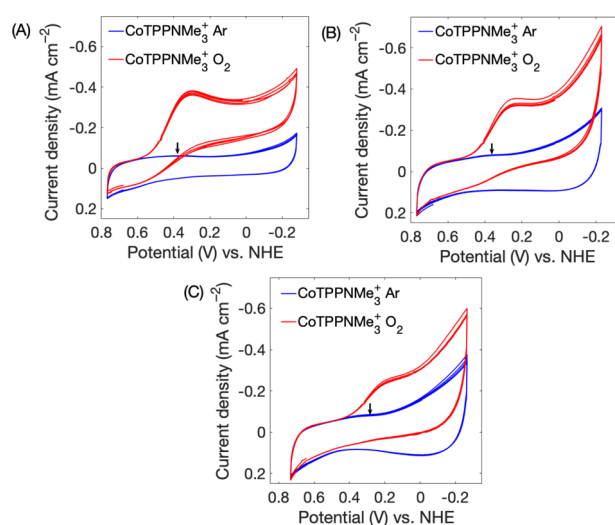


Figure 2. Cyclic voltammograms at pH 0 (A), pH 4 (B), and pH 7 (C) of CoTPPNMe₃⁺ drop-cast on EPG. Blue traces are in Ar-sparged solution and red are in O₂-sparged solution. All scan rates are 100 mV s⁻¹. The small vertical arrow indicates the position of $E_{p,c}$.

dependence of the Co^{III/II} couple is roughly consistent with the behavior of a soluble, related analog cobalt(5,10,15,20-tetra(4-N-methylpyridyl)porphyrin)^{65,66} where the pH-dependence is attributed to protonation/deprotonation of an axially ligated H₂O. For CoTPPNH₂ and CoTPPNMe₂, $E_{p,c}$ are observed at 0.32 and 0.38 V, respectively. CoTPPNMe₃⁺ has $E_{p,c}$ at 0.37 V. Notably, the $E_{p,c}$ values for CoTPPNMe₃⁺ are comparatively weakly dependent on pH, shifting ~50 mV more negative between pH 0 and 7. In cases where $E_{p,a}$ is clearly observed, the large peak separations are consistent with the large reorganization energy associated with the Co^{III/II} couple. Furthermore, weak current responses for CO-porphyrins can be attributed to the slow addition of axial ligands to Co^{III} sites in heterogeneous films.²⁵ We also note that the amount of catalyst that we deposit is higher than reports for other EPG-deposited Co-porphyrins,^{18,25,28} to enable direct comparison with our previous work.²⁶ Additional CVs for CoTPPNMe₃⁺ at 50% less loading are shown in the Supporting Information for comparison ([Figure S16](#)).

When the electrolyte solutions are sparged with O₂, CVs for all of the drop-cast Co-porphyrins show a definite increase in current near the Co^{III/II} couple ([Figure 3](#) and [Supporting Information Figures S11–S13](#)). The increase in current is known for CoTPP, which is an established O₂-to-H₂O₂ reduction catalyst.^{25,27} For CoTPP (100 mV s⁻¹ scan rate),

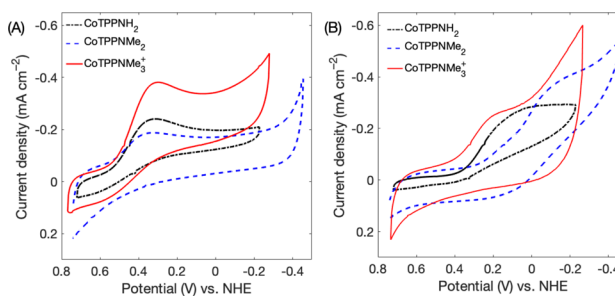


Figure 3. Comparison of cyclic voltammograms of EPG-adsorbed CoTPPNH₂ (black), CoTPPNMe₂ (blue), and CoTPPNMe₃⁺ (red) at pH 0 (A) and pH 7 (B). All scan rates are 100 mV s⁻¹.

the peak of the catalytic wave, or E_{cat} , appears at 0.25 V (pH 0), 0.11 V (pH 4) and -0.03 V (pH 7), or 40 mV per pH unit. For CoTPPNH₂, the E_{cat} is at 0.31 V (pH 0), 0.05 V (pH 4), -0.16 V (pH 7), or 67 mV per pH unit. The corresponding methylated complex, CoTPPNMe₂, shifts slightly more (ca. 75 mV per pH). Again, the CV behavior of CoTPPNMe₃⁺ (Figure 2) is distinct from the other Co-porphyrins. Catalytic currents are observed, but the maximum current values and E_{cat} positions are more weakly dependent on pH. From pH 0 to pH 7, the catalytic wave position moves about 0.18 V, or 26 mV per pH unit. In all cases, the observed current density is not systematically dependent on pH.

The pH dependence of the O₂/H₂O couple is 59 mV per pH, but the speciation of the Co-porphyrins will introduce additional pH dependences. First, axially ligated waters will introduce a pH dependence to the Co^{III/II} reduction potentials.^{65,66} In addition, the protonation state of CoTPPNH₂ and CoTPPNMe₂ will depend on pH. Using the pK_a values of aniline (pK_a = 4.6) and *N,N*-dimethylaniline (pK_a = 5.2) as models,⁶⁷ it is expected that CoTPPNH₂ and CoTPPNMe₂ are fully protonated at pH 0 and deprotonated at pH 7. Finally, changing the pH can affect the protonation states of surface groups on the graphite electrode,⁶⁸ which also could affect the Co^{III/II} couple.

The above results indicate that all of the newly tested Co-porphyrins are active ORR catalysts. Next, the products of O₂ reduction by each catalyst were analyzed using a series of hydrodynamic electrochemistry experiments. First, rotating ring-disk electrochemistry (RRDE) was used as a direct probe of the selectivity of ORR for each of the cobalt catalysts. As for the CV experiments, pH values of 0, 4, and 7 were used and the results are set out in Table 1. ORR selectivity was assayed

Table 1. Summary of the Number of Electrons (n) Involved in ORR Catalysis for Each Cobalt Porphyrin

Catalyst	pH	RRDE		RDE
		n_{RRDE}	H ₂ O%	n_{RDE}
CoTPP	0	2.6 ± 0.1	31 ± 5	2.2 ± 0.3
	4	2.8 ± 0.2	40 ± 5	2.3 ± 0.2
	7	3.0 ± 0.1	48 ± 5	2.6 ± 0.1
CoTPPNH ₂	0	3.1 ± 0.1	57 ± 4	3.5 ± 0.5
	4	2.7 ± 0.2	33 ± 5	3.1 ± 0.4
	7	3.0 ± 0.1	49 ± 6	2.2 ± 0.2
CoTPPNMe ₂	0	3.4 ± 0.1	68 ± 3	3.0 ± 0.5
	4	3.0 ± 0.1	51 ± 6	3.2 ± 0.4
	7	3.1 ± 0.1	54 ± 7	2.2 ± 0.2
CoTPPNMe ₃ ⁺	0	3.8 ± 0.2	91 ± 4	3.5 ± 0.2
	4	3.5 ± 0.2	74 ± 5	3.2 ± 0.3
	7	3.2 ± 0.2	62 ± 8	3.4 ± 0.4

by calculating the number of electrons (n) involved in ORR using eq 1

$$n = 4I_{\text{d}} \times (I_{\text{d}} + I_{\text{r}}/N)^{-1} \quad (1)$$

In eq 1, I_{d} is the EPG disk current, I_{r} is the Pt ring current, and N is the ring collection efficiency (0.24, as determined using potassium ferricyanide as a standard, see Supporting Information). The percent H₂O was calculated using equation S1 (see Supporting Information). RRDE traces for CoTPPNMe₃⁺ are set out in Figure 4 and are in available the Supporting Information for the other porphyrins. As expected, CoTPP catalyzes primarily a 2e⁻ O₂ reduction

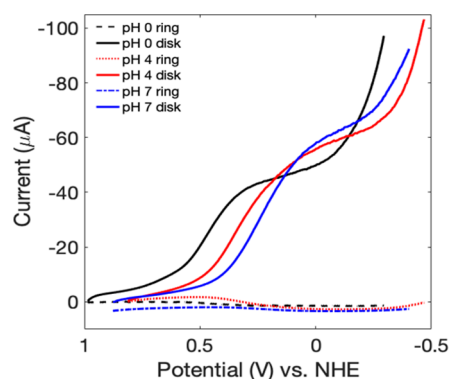


Figure 4. RRDE linear sweep voltammograms for CoTPPNMe₃⁺ deposited on an EPG disk electrode under 1 atm O₂. The rotation rate was 900 rpm. The scan rate was 20 mV s⁻¹. The potential at the Pt ring was 1.2 V.

reaction to yield H₂O₂. The addition of a protonatable nitrogen in CoTPPNH₂ and CoTPPNMe₂ somewhat increases the selectivity for reduction of O₂ to H₂O at low pH, but the selectivity begins to favor production of H₂O₂ as the pH is raised. In contrast, CoTPPNMe₃⁺ exhibits a greater degree of 4H⁺/4e⁻ O₂ reduction at all pH values tested.

We also carried out rotating disk electrochemistry (RDE) experiments and analyzed the results using Koutecky–Levich (K-L) analysis (eq 2, Figure 5) as an independent measure of the number of electrons involved in O₂ reduction. eq 2 is given as

$$i^{-1} = i_{\text{k}}^{-1} + (0.62nFAD^{2/3}\nu^{-1/6}C)^{-1} \times \omega^{-1/2} \quad (2)$$

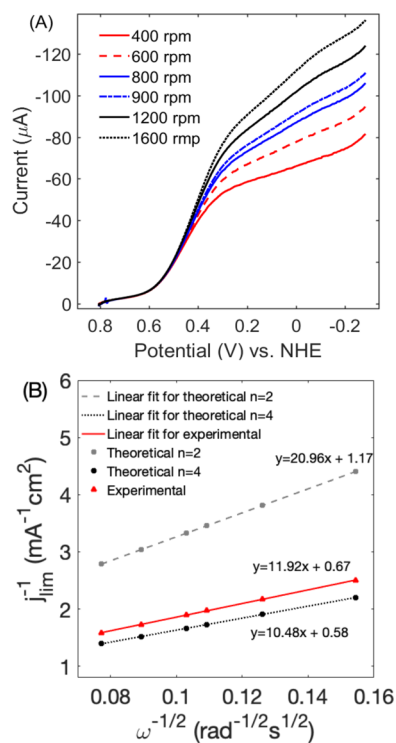


Figure 5. (A) Linear sweep voltammograms from rotating disk electrochemistry experiments for CoTPPNMe₃⁺ in pH 0 solution and (B) Koutecky–Levich (K-L) plots) derived from the data in panel (A).

where I is the observed current, n is the number of electrons passed, F is the Faraday constant (96485 C mol^{-1}), A is the electrode surface area (0.075 cm^2), D is the diffusion coefficient of O_2 ($1.9 \times 10^5 \text{ cm}^2 \text{ s}^{-1}$), ν is the kinematic viscosity of water (at $22 \text{ }^\circ\text{C} = 0.01 \text{ cm}^2 \text{ s}^{-1}$), C is the concentration of O_2 ($2.6 \times 10^{-7} \text{ mol cm}^3$),^{69,70} and ω is the electrode rotation rate in radians per second. K-L plots (e.g., Figure 5) were linear and the values calculated for n from the slopes of the linear fits are set out in Table 1. Additional K-L plots are shown in the Supporting Information.

The results for analyses using K-L plots are, in general, similar to those from RRDE. However, there are some differences, especially as the pH is increased for CoTPP, CoTPPNH₂ and CoTPPNMe₂. We are not the first to notice such behavior when comparing between RDE and RRDE experiments for Co-porphyrin catalyzed ORR.⁶⁴ In addition, RRDE experiments are sensitive to the state of the Pt ring electrode, especially when significant H_2O_2 is produced.²⁵ For CoTPP, n is less than 4 at all pH, consistent with other reports.^{25,27} In contrast, CoTPPNMe₃⁺ is much more selective for the reduction of O_2 to H_2O at all pH. For CoTPPNH₂ and CoTPPNMe₂, more H_2O is produced at pH 0 (when the ancillary group is protonated) than at pH 4 or 7. Based on marked differences in the shape of RDE traces as the pH is increased, these two catalysts appear to be less stable when more H_2O_2 is produced. One possibility is reactions of free or metal-catalyzed oxidations of the amine groups by the H_2O_2 produced during O_2 reduction.^{71–73} This may contribute to the disagreement between RDE and RRDE results at higher pH (Table 1). Based on these results, aniline and dimethylaniline groups appear to be satisfactory proton relays at low pH (i.e., when they are protonated), but their susceptibility to oxidation makes them unsuitable for systems where strong oxidants can be produced.

The kinetics of O_2 reduction by CoTPPNMe₃⁺ drop-cast on EPG electrodes in different pH solutions were extracted from K-L plots. The electroactive CoTPPNMe₃⁺ concentration on EPG electrodes were calculated from the total charge ($Q_{\text{CV}} = 155, 119, \text{ and } 90 \text{ nC}$ at pH 0, 4, and 7, respectively) passed at the reductive $\text{Co}^{\text{III/II}}$ in argon-sparged solutions, i.e., $\Gamma_{\text{cat}} = Q_{\text{CV}}/nFA$, where n was the number of electrons is 1, F was Faraday constant, and A was electrode surface area. The above charges yields values of Γ_{cat} of $2.1 \times 10^{-11} \text{ mol cm}^{-2}$, $1.6 \times 10^{-11} \text{ mol cm}^{-2}$ and $1.2 \times 10^{-11} \text{ mol cm}^{-2}$, respectively, at pH 0, 4, and 7. The intercepts from K-L plots were used to calculate the catalytic rate constants. The second-order catalytic rate constant for CoTPPNMe₃⁺ drop-cast on EPG were $1.1 \times 10^6, 9.3 \times 10^5, \text{ and } 9.1 \times 10^5 \text{ M}^{-1} \text{ s}^{-1}$ at pH 0, 4 and 7, respectively. These rates are very similar to those reported for other heterogeneous Co-porphyrin catalysts.^{64,74} Strikingly, the rate constants are nearly insensitive to pH between pH 0 and 7.

Turnover frequency (TOF)^{75,76} values were determined using the k_{cat} values given above and the concentration of O_2 in electrolytes under 1 atm of O_2 . A summary of different logTOF for each pH studied as a function of overpotential are shown in Figure 6. The logTOF values come from the different intercept values from K-L plots (see Supporting Information). The maximum values of TOF were observed between 0.8 and 1 V overpotential for all pH values. Again, it is noteworthy that the trends of logTOF versus overpotential are very similar across pH values of 0 to 7. Analogous plots for CoTPP, CoTPPNH₂, and CoTPPNMe₂ are not as informative since the product

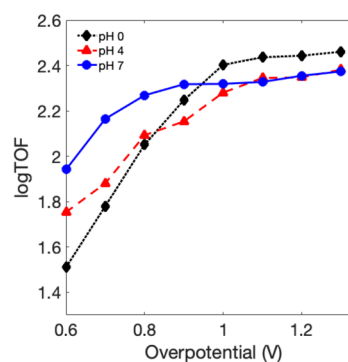


Figure 6. Turnover–overpotential relationships for CoTPPNMe₃⁺ at different pH values. TOF values were determined from K–L plots from RDE data collected in pH 0, 4, and 7 solutions under 1 atm O_2 .

selectivity (H_2O versus H_2O_2) changes with pH. Likewise, inspection of K-L plots for overpotentials lower than 0.6 for CoTPPNMe₃⁺ suggest an increase in H_2O_2 production, so those data are not shown in Figure 6.

Among the catalysts described here, and those in our previous work,²⁶ CoTPPNMe₃⁺ is unique. It lacks an explicit proton relay, yet catalyzes the $4\text{H}^+/4\text{e}^-$ reduction of O_2 with good rates and selectivity from pH 0 to 7. For CoTPPNH₂, CoTPPNMe₂, and two previously reported complexes CoTPOH and CoTPPy (5-(2-hydroxyphenyl)-10,15,20-triphenylporphyrinato cobalt(II) and 5-(2-pyridyl)-10,15,20-triphenylporphyrinato cobalt(II), respectively), we can begin by comparing relative pK_a values of the different proton relays. Again taking the aqueous pK_a values as models (i.e., pyridine (5.3), aniline (4.6), *N,N*-dimethylaniline (5.2) and phenol (10)⁶⁷) it is straightforward to see one reason why CoTPOH is the least effective ORR catalyst; the 2-hydroxyphenyl group is a much weaker acid and also cannot form a cation. Consistent with this idea is the behavior of the three Co-porphyrins with nitrogen bases, all of $pK_a \sim 5$. These catalysts have $n = 3–4$ for ORR at pH 0 (i.e., H_2O is the main product), but $n \sim 2$ at higher pH values. Notably, at pH 0 the selectivity of CoTPPy is quite similar to CoTPPNH₂ and CoTPPNMe₂, despite the different distance between the ionizable nitrogen and the metal. This has been commented on, and modeled, for a related iron porphyrin.¹³

Next, we consider reasons why CoTPPNMe₃⁺ shows better selectivity for reduction of O_2 to H_2O in comparison to the three other Co-porphyrins. As noted in the Introduction, the mechanism of ORR by Co-porphyrins has been proposed to proceed via reduction of a peroxide- or hydroperoxide-bound intermediates.³⁷ Our initial hypothesis was that the cationic trimethylaniline group would stabilize these intermediates and promote selectivity for reduction of O_2 to H_2O . To gain a greater level of insight into this proposal, we carried out quantum chemical calculations using the series of intermediates proposed by Anson.³⁷ The complexes considered were CoTPP, CoTPPNH₂ and CoTPPNMe₃⁺ with O_2 , O_2^{2-} , and HOO^- ligands. Optimized structures are given in the Supporting Information. Bond metrical parameters for CoTPP were in accord with experiment,^{51,52} and those for the CoTPP- O_2 complex were similar to other computational studies.^{77,78} Optimized structures and some key bond lengths are shown in Figure 7. For simplicity, only CoTPPNH₂ and CoTPPNMe₃⁺ are shown in Figure 7. The results for CoTPP are very similar to those for CoTPPNH₂ (see Supporting

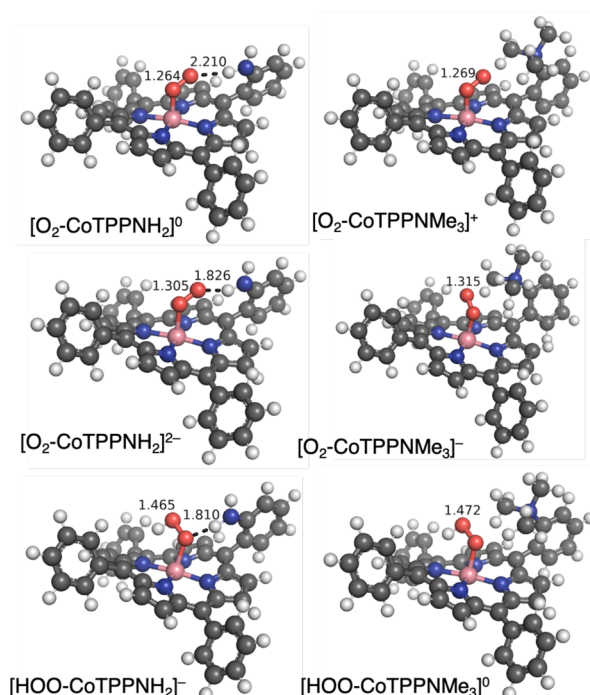


Figure 7. Optimized structures for CoTPPNH₂ (left column) and CoTPPNMe₃⁺ (right column). The top row shows dioxygen complexes, the middle row shows peroxide complexes, and the bottom row shows hydroperoxide complexes. The O–O distances are given above the oxygen ligands and the NH–O bond distances are given from CoTPPNH₂.

Information). The CoTPPNMe₃⁺ complex shows longer O–O bond lengths in each of the complexes in Figure 7. Notably, the O–O bond length in the hydroperoxide complex [HOO-CoTPPNMe₃]⁰ is longer than we calculated for H₂O₂ (1.472 Å versus 1.466 Å). This greater degree of activation is consistent with the observation that the CoTPPNMe₃⁺ reduction of O₂ to H₂O rather than H₂O₂.

Free energies were calculated for different reaction steps (Figure 8) following methods described by Carter and co-

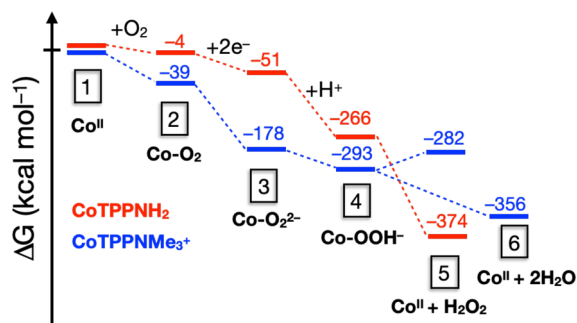


Figure 8. Calculated relative free energy changes for O₂ reduction by CoTPPNH₂ (red) and CoTPPNMe₃⁺ (blue).

workers.⁵⁶ The calculations suggest that hydrogen bond between bound O₂ and the anilino group slightly promotes the O₂ binding step (1 → 2). Interestingly, CoTPPNMe₃⁺ is calculated to have a higher affinity for O₂, likely via ionic stabilization of bound superoxide (i.e., a formally Co(III)-O₂^{•-} complex^{33–35}). Two electron reduction (2 → 3) to give a Co(II)-peroxide is more favorable for the CoTPPNMe₃⁺

complex. The subsequent protonation (3 → 4) of the dianionic CoTPP-peroxide complex, to give the corresponding Co-hydroperoxide complex, is more favorable for CoTPP and CoTPPNH₂, resulting in an energy that is relatively close to that for the CoTPPNMe₃⁺ hydroperoxide complex. Protonation of the CoTPPNMe₃⁺-hydroperoxide complex to give H₂O₂ is predicted to be unfavorable (4 → 5), while the pathway to yield H₂O is favored (4 → 6).

CONCLUSIONS

The development of catalysts for the oxygen reduction reaction (ORR) continues to be a challenge. The results presented here suggest that stabilization of intermediates through electrostatic interactions can play distinct roles in determining catalyst selectivity for reduction of O₂. The ORR selectivity of iron porphyrin catalysts can be improved by introduction of hydrogen bonding interactions that influence the chemistry of Fe(III)-OOH intermediates or O₂ binding events.^{16,17,32} One important example is the ORR selectivity over a wide range of pH values observed in a triazole-ferrocene modified Fe-porphyrin, which likely arises from an interplay of local hydrogen bonds and ferrocene-mediated ET.¹⁷ In contrast, cobalt porphyrin ORR catalysts cannot access high valent intermediates and therefore must proceed via a different mechanism. This leads to our proposal that ORR selectivity of Co-porphyrins can be improved by accounting for the mechanistic steps that are distinct from Fe-porphyrins. Instead of hydrogen bonding, electrostatic stabilization of anionic intermediates (likely peroxide-bound Co(II)) by conjugate acids of nitrogen bases, or trimethylanilinium (cationic) groups is important. We demonstrated that the use of a trimethylanilinium group proximal to the catalytic porphyrin-cobalt site results in pH-independence of ORR rates and overpotentials. We suggest that this could be an overlooked design element for ORR catalysts, and potentially for other redox catalysts. One example comes from the CO₂ reduction literature, where a cobalt phthalocyanine with a trimethylanilinium group is an effective catalyst,⁷⁹ though the mechanism there is less clear because the NMe₃⁺ group is not proximal to the Co. In sum, the unique physical properties of cobalt porphyrins mean that ORR occurs by a mechanism that is different than for iron porphyrins. This, in turn, demands different catalyst design elements. Ultimately, catalysts that operate over a wider range of reaction conditions, such as different pH ranges, can be envisioned by considering electrostatic interactions of activated intermediates.

ASSOCIATED CONTENT

Supporting Information

The Supporting Information is available free of charge on the ACS Publications Web site. The Supporting Information is available free of charge at <https://pubs.acs.org/doi/10.1021/jacs.0c03861>.

Additional experimental details and characterization data, additional cyclic voltammograms and corresponding analyses, controlled potential electrolysis traces, details of all calculations, and comparisons of catalyst performance under different conditions (PDF)

AUTHOR INFORMATION

Corresponding Author

Jeffrey J. Warren – Simon Fraser University, Department of Chemistry, Burnaby, BC V5A 1S6, Canada; orcid.org/0000-0002-1747-3029; Email: j.warren@sfu.ca

Author

Rui Zhang – Simon Fraser University, Department of Chemistry, Burnaby, BC V5A 1S6, Canada

Complete contact information is available at:

<https://pubs.acs.org/10.1021/jacs.0c03861>

Author Contributions

The manuscript was written through contributions of all authors. All authors have given approval to the final version of the manuscript.

Notes

The authors declare no competing financial interest.

ACKNOWLEDGMENTS

The Natural Sciences and Engineering Research Council (NSERC, RGPIN 05559 to J.J.W.) and Simon Fraser University are acknowledged for support. R.Z. is grateful for Ph.D. scholarship support from the China Scholarship Council. We are grateful for helpful discussions with Soumalya Sinha and Tim Storr. Calculations were enabled in part by support provided by (WestGrid) (www.westgrid.ca) and Compute Canada (www.computeCanada.ca)

REFERENCES

- (1) Rich, P. R.; Maréchal, A. The Mitochondrial Respiratory Chain. *Essays Biochem.* **2010**, *47*, 1–23.
- (2) Yoshikawa, S.; Shimada, A. Reaction Mechanism of Cytochrome *c* Oxidase. *Chem. Rev.* **2015**, *115* (4), 1936–1989.
- (3) Wikström, M.; Krab, K.; Sharma, V. Oxygen Activation and Energy Conservation by Cytochrome *c* Oxidase. *Chem. Rev.* **2018**, *118* (5), 2469–2490.
- (4) Debe, M. K. Electrocatalyst Approaches and Challenges for Automotive Fuel Cells. *Nature* **2012**, *486* (7401), 43–51.
- (5) Jaouen, F.; Proietti, E.; Lefèvre, M.; Chenitz, R.; Dodelet, J.-P.; Wu, G.; Chung, H. T.; Johnston, C. M.; Zelenay, P. Recent Advances in Non-Precious Metal Catalysis for Oxygen-Reduction Reaction in Polymer Electrolyte Fuelcells. *Energy Environ. Sci.* **2011**, *4* (1), 114–130.
- (6) Gewirth, A. A.; Varnell, J. A.; DiAscro, A. M. Nonprecious Metal Catalysts for Oxygen Reduction in Heterogeneous Aqueous Systems. *Chem. Rev.* **2018**, *118* (5), 2313–2339.
- (7) Pegis, M. L.; Wise, C. F.; Martin, D. J.; Mayer, J. M. Oxygen Reduction by Homogeneous Molecular Catalysts and Electrocatalysts. *Chem. Rev.* **2018**, *118* (5), 2340–2391.
- (8) Fukuzumi, S.; Mochizuki, S.; Tanaka, T. Efficient Reduction of Dioxygen with Ferrocene Derivatives, Catalyzed by Metalloporphyrins in the Presence of Perchloric Acid. *Inorg. Chem.* **1989**, *28* (12), 2459–2465.
- (9) Carver, C. T.; Matson, B. D.; Mayer, J. M. Electrocatalytic Oxygen Reduction by Iron Tetra-Arylporphyrins Bearing Pendant Proton Relays. *J. Am. Chem. Soc.* **2012**, *134* (12), 5444–5447.
- (10) Passard, G.; Dogutan, D. K.; Qiu, M.; Costentin, C.; Nocera, D. G. Oxygen Reduction Reaction Promoted by Manganese Porphyrins. *ACS Catal.* **2018**, *8* (9), 8671–8679.
- (11) Pegis, M. L.; Martin, D. J.; Wise, C. F.; Brezny, A. C.; Johnson, S. I.; Johnson, L. E.; Kumar, N.; Raugei, S.; Mayer, J. M. Mechanism of Catalytic O₂ Reduction by Iron Tetrphenylporphyrin. *J. Am. Chem. Soc.* **2019**, *141* (20), 8315–8326.
- (12) Costentin, C.; Dridi, H.; Savéant, J.-M. Molecular Catalysis of O₂ Reduction by Iron Porphyrins in Water: Heterogeneous versus Homogeneous Pathways. *J. Am. Chem. Soc.* **2015**, *137* (42), 13535–13544.
- (13) Matson, B. D.; Carver, C. T.; Von Ruden, A.; Yang, J. Y.; Raugei, S.; Mayer, J. M. Distant Protonated Pyridine Groups in Water-Soluble Iron Porphyrin Electrocatalysts Promote Selective Oxygen Reduction to Water. *Chem. Commun.* **2012**, *48* (90), 11100–11102.
- (14) Forshey, P. A.; Kuwana, T. Electrochemistry of Oxygen Reduction. 4. Oxygen to Water Conversion by Iron(II)(Tetrakis(N-Methyl-4-Pyridyl)Porphyrin) via Hydrogen Peroxide. *Inorg. Chem.* **1983**, *22* (5), 699–707.
- (15) Rosenthal, J.; Nocera, D. G. Role of Proton-Coupled Electron Transfer in O–O Bond Activation. *Acc. Chem. Res.* **2007**, *40*, 543–553.
- (16) Ghatak, A.; Bhakta, S.; Bhunia, S.; Dey, A. Influence of the Distal Guanidine Group on the Rate and Selectivity of O₂ Reduction by Iron Porphyrin. *Chem. Sci.* **2019**, *10* (42), 9692–9698.
- (17) Mitra, K.; Chatterjee, S.; Samanta, S.; Dey, A. Selective 4e⁻/4H⁺ O₂ Reduction by an Iron(Tetraferrocenyl)Porphyrin Complex: From Proton Transfer Followed by Electron Transfer in Organic Solvent to Proton Coupled Electron Transfer in Aqueous Medium. *Inorg. Chem.* **2013**, *52* (24), 14317–14325.
- (18) Shi, C.; Anson, F. C. Cobalt Meso-Tetrakis(N-Methyl-4-Pyridiniumyl)Porphyrin Becomes a Catalyst for the Electroreduction of O₂ by Four Electrons When [(NH₃)₅Os]ⁿ⁺ (n = 2, 3) Groups Are Coordinated to the Porphyrin Ring. *Inorg. Chem.* **1996**, *35* (26), 7928–7931.
- (19) Shi, C.; Anson, F. C. Electrocatalysis of the Reduction of Molecular Oxygen to Water by Tetraruthenated Cobalt Meso-Tetrakis(4-Pyridyl)Porphyrin Adsorbed on Graphite Electrodes. *Inorg. Chem.* **1992**, *31* (24), 5078–5083.
- (20) Collman, J. P. Synthetic Models for the Oxygen-Binding Hemoproteins. *Acc. Chem. Res.* **1977**, *10* (7), 265–272.
- (21) Collman, J. P.; Fu, L. Synthetic Models for Hemoglobin and Myoglobin. *Acc. Chem. Res.* **1999**, *32*, 455–463.
- (22) Collman, J. P.; Devaraj, N. K.; Decreau, R. A.; Yang, Y.; Yan, Y.-L.; Ebina, W.; Eberspacher, T. A.; Chidsey, C. E. D. A Cytochrome *c* Oxidase Model Catalyzes Oxygen to Water Reduction Under Rate-Limiting Electron Flux. *Science* **2007**, *315* (5818), 1565–1568.
- (23) Zhang, W.; Lai, W.; Cao, R. Energy-Related Small Molecule Activation Reactions: Oxygen Reduction and Hydrogen and Oxygen Evolution Reactions Catalyzed by Porphyrin- and Corrole-Based Systems. *Chem. Rev.* **2017**, *117* (4), 3717–3797.
- (24) Sinha, S.; Aaron, M. S.; Blagojevic, J.; Warren, J. J. Electrocatalytic Dioxygen Reduction by Carbon Electrodes Non-covalently Modified with Iron Porphyrin Complexes: Enhancements from a Single Proton Relay. *Chem. - Eur. J.* **2015**, *21* (50), 18072–18075.
- (25) Song, E.; Shi, C.; Anson, F. C. Comparison of the Behavior of Several Cobalt Porphyrins as Electrocatalysts for the Reduction of O₂ at Graphite Electrodes. *Langmuir* **1998**, *14* (15), 4315–4321.
- (26) Sinha, S.; Ghosh, M.; Warren, J. J. Changing the Selectivity of O₂ Reduction Catalysis with One Ligand Heteroatom. *ACS Catal.* **2019**, *9* (3), 2685–2691.
- (27) Yuasa, M.; Steiger, B.; Anson, F. C. Hydroxy-Substituted Cobalt Tetrphenylporphyrins as Electrocatalysts for the Reduction of O₂. *J. Porphyrins Phthalocyanines* **1997**, *1*, 181–188.
- (28) Yuasa, M.; Yamaguchi, A.; Oyaizu, K.; Fujito, Y.; Kitao, M.; Sato, T. Cobaltporphyrin-Adsorbed Carbon Black: Highly Efficient Electrocatalysts for Oxygen Reduction. *Polym. Adv. Technol.* **2005**, *16* (9), 702–705.
- (29) Shi, C.; Steiger, B.; Yuasa, M.; Anson, F. C. Electroreduction of O₂ to H₂O at Unusually Positive Potentials Catalyzed by the Simplest of the Cobalt Porphyrins. *Inorg. Chem.* **1997**, *36* (20), 4294–4295.
- (30) Costentin, C.; Savéant, J.-M. Towards an Intelligent Design of Molecular Electrocatalysts. *Nat. Rev. Chem.* **2017**, *1* (11), 0087.

- (31) Sengupta, K.; Chatterjee, S.; Samanta, S.; Dey, A. Direct Observation of Intermediates Formed during Steady-State Electro-catalytic O₂ Reduction by Iron Porphyrins. *Proc. Natl. Acad. Sci. U. S. A.* **2013**, *110* (21), 8431–8436.
- (32) Bhunia, S.; Rana, A.; Roy, P.; Martin, D. J.; Pegis, M. L.; Roy, B.; Dey, A. Rational Design of Mononuclear Iron Porphyrins for Facile and Selective 4e⁻/4H⁺ O₂ Reduction: Activation of O–O Bond by 2nd Sphere Hydrogen Bonding. *J. Am. Chem. Soc.* **2018**, *140* (30), 9444–9457.
- (33) Walker, F. A. Electron Spin Resonance Study of Coordination to the Fifth and Sixth Positions of $\alpha,\beta,\gamma,\delta$ -Tetra(p-Methoxyphenyl)-Porphinatocobalt(II). *J. Am. Chem. Soc.* **1970**, *92* (14), 4235–4244.
- (34) Walker, F. Ann. Reactions of Monomeric Cobalt-Oxygen Complexes. I. Thermodynamics of Reaction of Molecular Oxygen with Five- and Six-Coordinate Amine Complexes of a Cobalt Porphyrin. *J. Am. Chem. Soc.* **1973**, *95* (4), 1154–1159.
- (35) Collman, J. P.; Yan, Y.-L.; Eberspacher, T.; Xie, X.; Solomon, E. I. Oxygen Binding of Water-Soluble Cobalt Porphyrins in Aqueous Solution. *Inorg. Chem.* **2005**, *44* (26), 9628–9630.
- (36) Winkler, J. R.; Gray, H. B. Electronic Structures of Oxo-Metal Ions. In *Molecular Electronic Structures of Transition Metal Complexes I*; Mingos, D. M. P., Day, P., Dahl, J. P., Eds.; Structure and Bonding; Springer: Berlin, Heidelberg, 2012; pp 17–28. DOI: 10.1007/430_2011_55.
- (37) Durand, R. R.; Anson, F. C. Catalysis of Dioxygen Reduction at Graphite Electrodes by an Adsorbed Cobalt(II) Porphyrin. *J. Electroanal. Chem. Interfacial Electrochem.* **1982**, *134* (2), 273–289.
- (38) Rigby, M. L.; Wasylenko, D. J.; Pegis, M. L.; Mayer, J. M. Medium Effects Are as Important as Catalyst Design for Selectivity in Electro-catalytic Oxygen Reduction by Iron-Porphyrin Complexes. *J. Am. Chem. Soc.* **2015**, *137* (13), 4296–4299.
- (39) Azcarate, I.; Costentin, C.; Robert, M.; Savéant, J.-M. Through-Space Charge Interaction Substituent Effects in Molecular Catalysis Leading to the Design of the Most Efficient Catalyst of CO₂ -to-CO Electrochemical Conversion. *J. Am. Chem. Soc.* **2016**, *138* (51), 16639–16644.
- (40) Martin, D. J.; Mercado, B. Q.; Mayer, J. M. Combining Scaling Relationships Overcomes Rate versus Overpotential Trade-Offs in O₂ Molecular Electrocatalysis. *Sci. Adv.* **2020**, *6* (11), No. eaaz3318.
- (41) Hanson, S. S.; Warren, J. J. Syntheses, Characterization, and Electrochemical Behavior of Alkylated 2-(2'-Quinolybenzimidazole) Complexes of Rhenium (I). *Can. J. Chem.* **2018**, *96* (2), 119–123.
- (42) Nichols, E. M.; Derrick, J. S.; Nistanaki, S. K.; Smith, P. T.; Chang, C. J. Positional Effects of Second-Sphere Amide Pendants on Electrochemical CO₂ Reduction Catalyzed by Iron Porphyrins. *Chem. Sci.* **2018**, *9* (11), 2952–2960.
- (43) Neese, F. The ORCA Program System. *Wiley Interdiscip. Rev.: Comput. Mol. Sci.* **2012**, *2*, 73–78.
- (44) Neese, F. Software Update: The ORCA Program System, Version 4.0. *Wiley Interdiscip. Rev.: Comput. Mol. Sci.* **2018**, *8* (1), No. e1327.
- (45) Tao, J.; Perdew, J. P.; Staroverov, V. N.; Scuseria, G. E. Climbing the Density Functional Ladder: Nonempirical Meta-Generalized Gradient Approximation Designed for Molecules and Solids. *Phys. Rev. Lett.* **2003**, *91* (14), 146401.
- (46) Neese, F.; Wennmohs, F.; Hansen, A.; Becker, U. Efficient, Approximate and Parallel Hartree-Fock and Hybrid DFT Calculations. A 'Chain-of-Spheres' Algorithm for the Hartree-Fock Exchange. *Chem. Phys.* **2009**, *356* (1), 98–109.
- (47) Stoychev, G. L.; Auer, A. A.; Neese, F. Automatic Generation of Auxiliary Basis Sets. *J. Chem. Theory Comput.* **2017**, *13* (2), 554–562.
- (48) Weigend, F. Accurate Coulomb-Fitting Basis Sets for H to Rn. *Phys. Chem. Chem. Phys.* **2006**, *8* (9), 1057–1065.
- (49) Grimme, S.; Antony, J.; Ehrlich, S.; Krieg, H. A Consistent and Accurate Ab Initio Parametrization of Density Functional Dispersion Correction (DFT-D) for the 94 Elements H–Pu. *J. Chem. Phys.* **2010**, *132* (15), 154104.
- (50) Grimme, S.; Ehrlich, S.; Goerigk, L. Effect of the Damping Function in Dispersion Corrected Density Functional Theory. *J. Comput. Chem.* **2011**, *32* (7), 1456–1465.
- (51) Nascimento, B. F. O.; Pineiro, M.; Rocha Gonsalves, A. M. d'A.; Ramos Silva, M.; Matos Beja, A.; Paixão, J. A. Microwave-Assisted Synthesis of Porphyrins and Metalloporphyrins: A Rapid and Efficient Synthetic Method. *J. Porphyrins Phthalocyanines* **2007**, *11* (02), 77–84.
- (52) Stevens, E. D. Electronic Structure of Metalloporphyrins. 1. Experimental Electron Density Distribution of (Meso-Tetraphenylporphinato)Cobalt(II). *J. Am. Chem. Soc.* **1981**, *103* (17), 5087–5095.
- (53) Balabanov, N. B.; Peterson, K. A. Systematically Convergent Basis Sets for Transition Metals. I. All-Electron Correlation Consistent Basis Sets for the 3d Elements Sc–Zn. *J. Chem. Phys.* **2005**, *123* (6), 064107.
- (54) Balabanov, N. B.; Peterson, K. A. Basis Set Limit Electronic Excitation Energies, Ionization Potentials, and Electron Affinities for the 3d Transition Metal Atoms: Coupled Cluster and Multireference Methods. *J. Chem. Phys.* **2006**, *125* (7), 074110.
- (55) Cossi, M.; Rega, N.; Scalmani, G.; Barone, V. Energies, Structures, and Electronic Properties of Molecules in Solution with the C-PCM Solvation Model. *J. Comput. Chem.* **2003**, *24* (6), 669–681.
- (56) Riplinger, C.; Sampson, M. D.; Ritzmann, A. M.; Kubiak, C. P.; Carter, E. A. Mechanistic Contrasts between Manganese and Rhenium Bipyridine Electrocatalysts for the Reduction of Carbon Dioxide. *J. Am. Chem. Soc.* **2014**, *136*, 16285–16298.
- (57) Keith, J. A.; Carter, E. A. Theoretical Insights into Pyridinium-Based Photoelectrocatalytic Reduction of CO₂. *J. Am. Chem. Soc.* **2012**, *134* (18), 7580–7583.
- (58) Tissandier, M. D.; Cowen, K. A.; Feng, W. Y.; Gundlach, E.; Cohen, M. H.; Earhart, A. D.; Coe, J. V.; Tuttle, T. R. The Proton's Absolute Aqueous Enthalpy and Gibbs Free Energy of Solvation from Cluster-Ion Solvation Data. *J. Phys. Chem. A* **1998**, *102* (40), 7787–7794.
- (59) Fifen, J. J.; Dhaouadi, Z.; Nsangou, M. Revision of the Thermodynamics of the Proton in Gas Phase. *J. Phys. Chem. A* **2014**, *118* (46), 11090–11097.
- (60) Ise, A. A.; Gennaro, A. Absolute Potential of the Standard Hydrogen Electrode and the Problem of Interconversion of Potentials in Different Solvents. *J. Phys. Chem. B* **2010**, *114* (23), 7894–7899.
- (61) Mu, X. H.; Kadish, K. M. Oxidative Electrochemistry of Cobalt Tetraphenylporphyrin under a CO Atmosphere. Interaction between Carbon Monoxide and Electrogenerated [(TPP)Co]⁺ in Nonbonding Media. *Inorg. Chem.* **1989**, *28* (19), 3743–3747.
- (62) Truxillo, L. A.; Davis, D. G. Electrochemistry of Cobalt Tetraphenylporphyrin in Aprotic Media. *Anal. Chem.* **1975**, *47* (13), 2260–2267.
- (63) Zhu, X.-Q.; Li, Q.; Hao, W.-F.; Cheng, J.-P. Dissociation Energies and Charge Distribution of the Co–NO Bond for Nitrosyl- $\alpha,\beta,\gamma,\delta$ -Tetraphenylporphinatocobalt(II) and Nitrosyl- $\alpha,\beta,\gamma,\delta$ -Tetraphenylporphinatocobalt(III) in Benzonitrile Solution. *J. Am. Chem. Soc.* **2002**, *124* (33), 9887–9893.
- (64) Zhang, W.; Shaikh, A. U.; Tsui, E. Y.; Swager, T. M. Cobalt Porphyrin Functionalized Carbon Nanotubes for Oxygen Reduction. *Chem. Mater.* **2009**, *21* (14), 3234–3241.
- (65) Pasternack, R. F.; Cobb, M. A. The Substitution Reactions of a Water Soluble Cobalt(III) Porphyrin with Thiocyanate as a Function of pH. *J. Inorg. Nucl. Chem.* **1973**, *35* (12), 4327–4339.
- (66) Chan, R. J. H.; Su, Y. O.; Kuwana, T. Electrocatalysis of Oxygen Reduction. 5. Oxygen to Hydrogen Peroxide Conversion by Cobalt(II) Tetrakis(N-Methyl-4-Pyridyl)Porphyrin. *Inorg. Chem.* **1985**, *24* (23), 3777–3784.
- (67) March, J. *Advanced Organic Chemistry*; John Wiley and sons: 1985; Vol. 3rd Ed.
- (68) Jackson, M. N.; Pegis, M. L.; Surendranath, Y. Graphite-Conjugated Acids Reveal a Molecular Framework for Proton-Coupled

Electron Transfer at Electrode Surfaces. *ACS Cent. Sci.* **2019**, acscentsci.9b00114. DOI: 10.1021/acscentsci.9b00114.

(69) Schöfberger, W.; Faschinger, F.; Chattopadhyay, S.; Bhakta, S.; Mondal, B.; Elemans, J. A. A. W.; Müllegger, S.; Tebi, S.; Koch, R.; Klappenberger, F.; Paszkiewicz, M.; Barth, J. V.; Rauls, E.; Aldahhak, H.; Schmidt, W. G.; Dey, A. A Bifunctional Electrocatalyst for Oxygen Evolution and Oxygen Reduction Reactions in Water. *Angew. Chem., Int. Ed.* **2016**, *55* (7), 2350–2355.

(70) Chatterjee, S.; Sengupta, K.; Hematian, S.; Karlin, K. D.; Dey, A. Electrocatalytic O₂-Reduction by Synthetic Cytochrome *c* Oxidase Mimics: Identification of a “Bridging Peroxo” Intermediate Involved in Facile 4e⁻/4H⁺ O₂-Reduction. *J. Am. Chem. Soc.* **2015**, *137* (40), 12897–12905.

(71) Cunningham, I. D.; Bachelor, J. L.; Pratt, J. M. Kinetic Study of the H₂O₂ Oxidation of Phenols, Naphthols and Anilines Catalysed by the Haem Octapeptide Microperoxidase-8. *J. Chem. Soc., Perkin Trans. 2* **1991**, *0* (11), 1839–1843.

(72) Howe, G. R.; Hiatt, R. R. Metal-Catalyzed Hydroperoxide Reactions. I. Substituent Effects in the Oxidation of Aniline. *J. Org. Chem.* **1970**, *35* (12), 4007–4012.

(73) Sheng, M. N.; Zajacek, J. G. Hydroperoxide Oxidations Catalyzed by Metals. II. Oxidation of Tertiary Amines to Amine Oxides. *J. Org. Chem.* **1968**, *33* (2), 588–590.

(74) Kadish, K. M.; Frémond, L.; Ou, Z.; Shao, J.; Shi, C.; Anson, F. C.; Burdet, F.; Gros, C. P.; Barbe, J.-M.; Guilard, R. Cobalt(III) Corroles as Electrocatalysts for the Reduction of Dioxygen: Reactivity of a Monocorrole, Biscorroles, and Porphyrin-Corrole Dyads. *J. Am. Chem. Soc.* **2005**, *127* (15), 5625–5631.

(75) Costentin, C.; Drouet, S.; Robert, M.; Savéant, J.-M. Turnover Numbers, Turnover Frequencies, and Overpotential in Molecular Catalysis of Electrochemical Reactions. Cyclic Voltammetry and Preparative-Scale Electrolysis. *J. Am. Chem. Soc.* **2012**, *134* (27), 11235–11242.

(76) Boudart, M. Turnover Rates in Heterogeneous Catalysis. *Chem. Rev.* **1995**, *95* (3), 661–666.

(77) Shi, Z.; Zhang, J. Density Functional Theory Study of Transitional Metal Macrocyclic Complexes' Dioxygen-Binding Abilities and Their Catalytic Activities toward Oxygen Reduction Reaction. *J. Phys. Chem. C* **2007**, *111* (19), 7084–7090.

(78) Sun, S.; Jiang, N.; Xia, D. Density Functional Theory Study of the Oxygen Reduction Reaction on Metalloporphyrins and Metallophthalocyanines. *J. Phys. Chem. C* **2011**, *115* (19), 9511–9517.

(79) Wang, M.; Torbensen, K.; Salvatore, D.; Ren, S.; Joulié, D.; Dumoulin, F.; Mendoza, D.; Lassalle-Kaiser, B.; Işci, U.; Berlinguette, C. P.; Robert, M. CO₂ Electrochemical Catalytic Reduction with a Highly Active Cobalt Phthalocyanine. *Nat. Commun.* **2019**, *10* (1), 1–8.